BIOCHEMISTRY
including biophysical chemistry & molecular biology

Rapid Report

pubs.acs.org/biochemistry

Entrapment of a Histone Tail by a DNA Lesion in a Nucleosome Suggests the Lesion Impacts Epigenetic Marking: A Molecular Dynamics Study

Iwen Fu,[†] Yuqin Cai,[†] Yingkai Zhang,[‡,§] Nicholas E. Geacintov,[‡] and Suse Broyde*[,†]

[†]Department of Biology and [‡]Department of Chemistry, New York University, New York, New York 10003, United States
[§]NYU-ECNU Center for Computational Chemistry at NYU Shanghai, Shanghai 200062, China

Supporting Information

ABSTRACT: Errors in epigenetic markings are associated with human diseases, including cancer. We have used molecular dynamics simulations of a nucleosome containing the 10*S* (+)-*trans*-*anti*-B[*a*]P-N^2-dG lesion, derived from the environmental pro-carcinogen benzo[*a*]pyrene, to elucidate the impact of the lesion on the structure and dynamics of a nearby histone N-terminal tail. Our results show that a lysine-containing part of this H2B tail that is subject to post-translational modification is engulfed by the enlarged DNA minor groove imposed by the lesion. The tail entrapment suggests that epigenetic markings could be hampered by this lesion, thereby impacting critical cellular functions, including transcription and repair.

The DNA histone N-terminal tails in nucleosomes have attracted much attention because post-translational modifications (PTMs) to these tails, which constitute epigenetic marks, modulate interactions between histones and DNA. Thereby, they regulate nucleosome stability. They also have an impact on chromatin compaction by controlling interactions between nucleosomes to form higher-order structures. By diminishing chromatin compaction and weakening histone−DNA interactions, post-translational modifications facilitate the access of DNA-binding proteins that regulate biological processes.[1−7] The modified histones also recruit other proteins[7] to control functions that include transcriptional regulation,[8−10] cell cycle progression,[5,11] and base[12,13] and nucleotide[14−17] excision repair (BER and NER, respectively). For example, it has been shown that the tails of histones H2A and H3 play key roles in coordinating BER by regulating expression of the critical BER glycosylase enzyme that is induced by methylmethane-sulfonate (MMS)-induced DNA lesions, with the absence of the tails leading to MMS hypersensitivity.[12]

Acetylation of lysine residues, which removes the positive charge from the ε-amino group of the lysines within the histone N-terminal tail, is one of the prominent and well-studied post-translational modifications of all histone tails and has important regulatory functions in transcription[9,10] and DNA repair.[1,5,8,18,19]

Errors in such epigenetic markings are associated with human diseases, including cancer,[20] inflammatory diseases,[21] and Huntington's disease.[22] Hyperacetylation of histone tails in lightly packed euchromatin is associated with transcription activation, while hypoacetylation of the tails in tightly packed

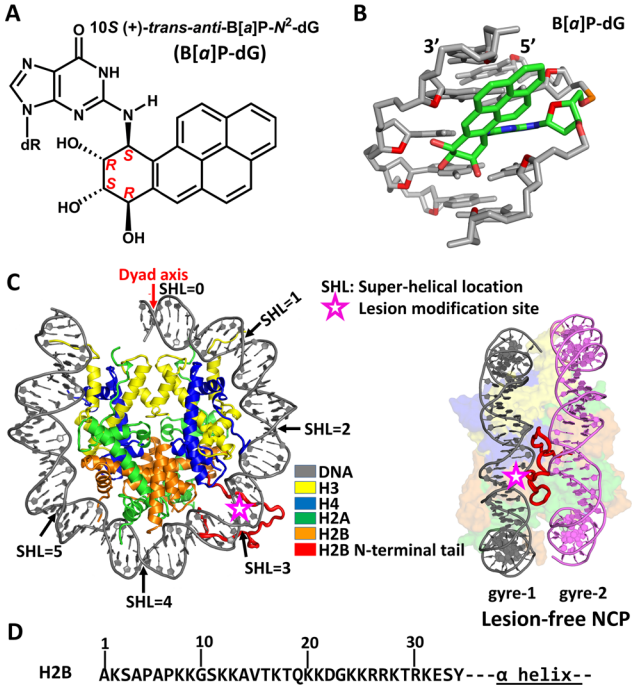

Figure 1. Lesion and nucleosome structures. (A) Chemical structure of the B[*a*]P-dG lesion investigated. (B) NMR solution structure of the B[*a*]P-dG lesion.[27] The B[*a*]P ring system is oriented in the 5′-direction of the modified strand, and the Watson−Crick pairing at the lesion site is maintained. The central 5-mer is shown. The DNA is colored gray with the O4′ atom colored red; the B[*a*]P-dG residue is colored by atom with carbon in green, oxygen red, and nitrogen blue. (C) Best representative structure (Movie S1) from our MD simulation of the lesion-free NCP with the H2B N-terminal tail at SHL ∼ 2.5−3.[31,32] Shown is the NCP viewed from the top (left) and side (right). At the dyad axis, which is at the center of the 145 bp DNA duplex, the SHL is 0. (D) Sequence of the H2B N-terminal tail. The residue numbering corresponds to the numbers in chain D of the crystal structure with PDB[30] entry 1KX5.[32]

Received: October 26, 2015
Revised: December 21, 2015

DOI: 10.1021/acs.biochem.5b01166
Biochemistry XXXX, XXX, XXX−XXX

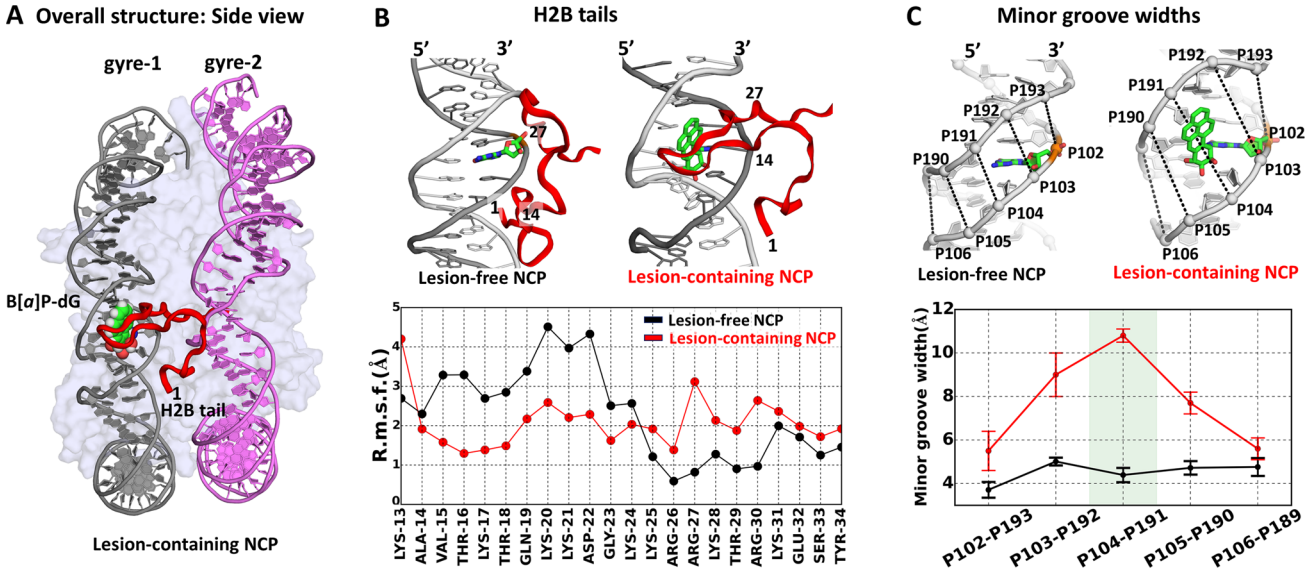

Figure 2. The histone H2B tail is locally less dynamic in the lesion-containing NCP than in the lesion-free NCP because the minor groove is enlarged, which allows entrapment of the tail. (A) Best representative structure (Movie S1) for the lesion-containing NCP. See Figure 1C (right panel) for a comparable view of lesion-free NCP. (B) Top panel: close-up view of the H2B tail and its surrounding DNA duplex containing the lesion, compared to the corresponding region in the lesion-free case. In A and B, the H2B tail is colored red, and residue numbers starting from the N-terminus are labeled. The bottom panel shows a comparison of the ensemble average values of rms fluctuations as a function of H2B tail residue numbers and their corresponding identities. (C) Top panel: minor groove widths around the lesion site are designated and are distances between backbone phosphates P103 and P192, P104 and P191, P105 and P190, etc., minus 5.8 Å to account for the van der Waals radius of the P atoms.[39] The bottom panel shows the ensemble average values of minor groove widths with block average standard deviations[40,41] for the lesion-containing NCP (red) and its lesion-free counterpart (black). The B[*a*]P-dG remains 5′-oriented as in the NMR solution structure[27] with Watson−Crick pairs maintained (Figure 1B). Color code is by atom with carbon green, oxygen red, nitrogen blue, and hydrogen white. In panel A, the B[*a*]P ring system is rendered as spheres; in panels B and C, the B[*a*]P-dG lesion and its corresponding unmodified nucleoside are rendered as sticks, with hydrogen atoms not displayed for the sake of clarity. See Figure S2 for correspondence between nucleotide numbers here (B and C) and the crystal structure with PDB[30] entry 2NZD.[31]

heterochromatin is associated with transcription repression.[10,23] A recent computational study has investigated the dynamics of nucleosome tails to elucidate how modifications by lysine acetylation impact chromatin compaction and unfolding.[24] Lysine acetyl modifications also function as docking sites for the recruitment of other proteins[7] to promote or repress transcription and repair.[9,10,13,15]

Experimental studies in yeast have demonstrated that deletion of histone H2B N-terminal tail residues 30−37 results in reduced NER efficiency and contributes to increased UV sensitivity, and that tail deletion mutants have increased nucleosome accessibility and mobility as shown by nuclease digestion studies.[25] Deletion of the H2B tail upregulates a large number of genes, suggesting that this tail can repress transcription.[26] A study with human HeLa cells showed that the H2B tail in its unacetylated state at Lys20 binds tumor suppressor p14ARF and thereby mediates transcription repression of cell cycle regulatory genes, which is lifted by tail acetylation.[11]

Our goal in the present work was to understand whether a DNA lesion impacts the structure and dynamics of a nearby histone tail. We investigated the minor groove-situated 10*S* (+)-*trans*-*anti*-B[*a*]P-N^2-dG[27] (B[*a*]P-dG) lesion (Figure 1A,B). This is the major and most mutagenic DNA lesion, derived from the carcinogenic environmental pollutant benzo[*a*]pyrene (B[*a*]P),[28] and it widens the DNA minor groove.[29] Simulations based on a nucleosome crystal structure with truncated tails (PDB[30] entry 2NZD[31]) showed that the lesion placed at superhelical location (SHL) ∼ 3, which is near to midway between the dyad and one end of the nucleosomal DNA duplex (Figure 1C), attracted the nearby stub of the H2B tail (Methods, Table S1, and Figure S1 of the Supporting Information). This observation suggested investigating the lesion's impact on this full-length H2B tail. To do so, we utilized the crystal structure that contains the full-length tails, with PDB[30] entry 1KX5.[32] In this structure, this H2B tail protrudes from the nucleosome core and is housed between the two DNA gyres at SHL ∼ 2.5−3. We restored the truncated H2B tail in the lesion-containing nucleosome to its full length (shown in Figure 1C) based on its structure in PDB entry 1KX5.[32] The full-length tail-containing nucleosome has the same *Xenopus laevis* histones as the one with truncated tails (sequence in Figure 1D). The local DNA 9-mer sequence context containing the lesion in the center is given in Figure S2 of the Supporting Information.

For this lesion-containing system with the full-length H2B tail, we conducted an 800 ns MD simulation using the AMBER14 package[33] with force fields ff99SB[34] for proteins and parmbsco[35] for DNA. We used the TIP3P[36] explicit water model and added K^+ to neutralize the charges. We also simulated a lesion-free control nucleosome with a full-length H2B tail for 800 ns to compare the effects of the lesion on the histone H2B tail. The combined 1D and 2D rmsds (Figures S3 and S4) showed that stable conformational states had been achieved after ∼300 ns in both cases. Full details concerning molecular modeling, force field, MD simulation protocol, and structural analyses are given in the Methods section of the Supporting Information. PyMOL (The PyMOL Molecular Graphic System, version 1.3.x, Schrodinger, LLC) and VMD[37]

DOI: 10.1021/acs.biochem.5b01166
Biochemistry XXXX, XXX, XXX−XXX

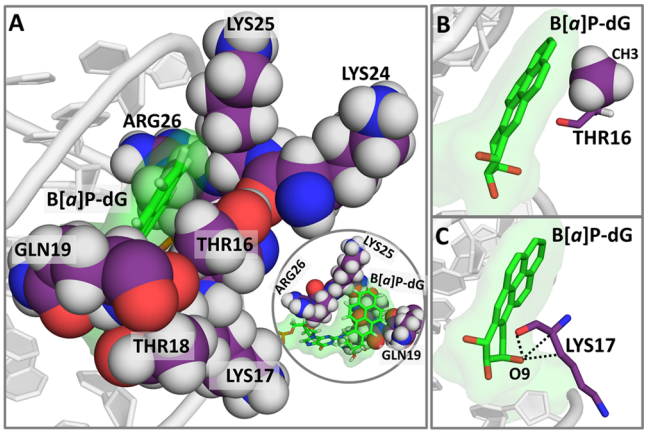

Figure 3. The H2B tail is entrapped in the minor groove by the B[*a*]P-dG lesion through a network of interactions. (A) The B[*a*]P-dG ring system is surrounded by H2B tail residues 16−26. Details of interactions are given in the Supporting Information. A view looking down the B[*a*]P-dG aromatic ring system is circled; Thr16 is beneath the B[*a*]P rings. (B) Me−π interactions[38] between the Thr16 methyl group and the B[*a*]P-dG aromatic ring system. (C) Hydrogen bond interactions, both conventional and carbon−oxygen,[42] between Lys17 and the B[*a*]P-dG O9 hydroxyl group are designated by dashed lines (see Figure S9 for full details). The DNA is gray, and all other residues are colored by atom with carbons purple for amino acids and green for the B[*a*]P-dG lesion. Hydrogens are white. The B[*a*]P-dG is rendered as both sticks and half-transparency surface. The amino acids are rendered as spheres in A with hydrogens displayed. The Arg26 hydrogens appear green because of the green veil from the half-transparency surface of the B[*a*]P-dG. In B, the Thr16 is in sticks, except the CH3 group which is in spheres. In C, Lys17 is in sticks. In B and C, the hydrogens are not displayed except for the CH3 group of Thr16. See Movie S1.

(Visual Molecular Dynamics, version 1.8.7) were employed for molecular modeling, images, and movies.

Our results showed a striking effect of the lesion on the positioning of the H2B tail and its dynamic properties (Figure 2B and Figure S5). In the lesion-free case, the H2B tail is housed between the two DNA gyres of the nucleosome (Figure 1C and Figure S5A). However, a notable rearrangement of the tail occurs in the presence of the B[*a*]P ring system (Figure 2A and Figure S5B), in that the tail becomes embedded in the groove. This occurs because the B[*a*]P rings widen the minor groove, which allows the tail to become entrapped and its mobility suppressed (Figure 2B). The locally diminished dynamics of the tail is revealed in its rms fluctuations (fluctuations in rmsd), which are much lower than in the lesion-free nucleosome up to Lys24. Beyond this point, the rms fluctuations are higher in the tail. The reason for the higher mobility comes from a change in the interactions of residues 26−30 (Arg26, Arg27, Lys28, Thr29, and Arg30) when the tail becomes embedded in the minor groove. In the lesion-free NCP, these residues are stably hydrogen bonded with bases and the backbone of the two DNA gyres, with occupancies of >95% (Table S2). When the tail becomes trapped by the lesion in the minor groove, most of these hydrogen bonds are ruptured and replaced by different hydrogen bonds with the DNA backbone that are fewer in number and weaker [occupancies mainly lower than 50% (Table S3)].

The widening of the minor groove by the B[*a*]P ring system is shown in Figure 2C, which presents a comparison of the minor groove structures and dimensions for the lesion-containing NCP and the lesion-free one. In the lesion-containing NCP, the groove at its maximal width is ∼11 Å, while in the lesion-free NCP, it is ∼4 Å, revealing a maximal groove enlargement of ∼7 Å. To determine how the entrapment of the tail impacts the minor groove dimensions, we compared the minor groove dimensions for the simulations of lesion-containing nucleosomes with full-length and truncated tails (Methods in the Supporting Information). Our results showed that the entrapped full-length tail enlarges the groove by only ∼1 Å, indicating that the enlargement of the minor groove results mainly from the B[*a*]P ring system (Figure S6).

A network of van der Waals interactions (Figures S7 and S8) and hydrogen bonds (Table S4) between amino acids of the tail with the B[*a*]P ring system and the adjacent DNA backbone is responsible for the tail entrapment (Figure 3A). The contact pattern revealed in this entrapment is dominated by the backbones of amino acids (Thr16, Lys17, Thr18, and Gln19) that are attracted by the B[*a*]P aromatic rings and its hydroxyl groups, while their side chains point away from the B[*a*]P ring system (Figure S7C). Also, the Thr16 methyl group (Me) makes favorable Me−π interactions[38] with the B[*a*]P aromatic rings (Figure 3B). Furthermore, Lys17 forms hydrogen bonds with the B[*a*]P benzylic ring O9 hydroxyl group (Figure 3C) and adjacent DNA backbone phosphate groups (Figure S9). In addition, internal hydrogen bonds between the backbones of histone H2B tail residues 14−24 stabilize the conformation of the entrapped tail (Table S5 and Figure S10).

The results obtained in the case of this example suggest that acetylation of Lys17, equivalent to Lys20 in the human H2B tail (see Figure S11), could be inhibited by the presence of the nearby minor groove lesion through the entrapment of the tail. Notably, the tail region that we found entrapped contains a number of lysines (Figure 1D), and one could envision that the acetylation of any or all of them could be inhibited by the lesion. Indeed, because of the flexibility of the side chains of the tail and its rich lysine content (Figure 1D), other arrangements of the entrapped tail involving interactions between lysines and other nearby amino acids with the lesion and local DNA backbone are plausible. In our simulation of the lesion-free nucleosome, the tail is more flexible, not embedded in the groove (Figure 2B) and available for acetylation. In addition, our work suggests that other lesions that greatly distort the minor groove could likewise entrap a histone tail.

More broadly, our work suggests the hypothesis that DNA lesions may play a role in fostering or impeding histone post-translational modifications and other functions of the tails, including their role in mediating internucleosomal interactions,[1] and thereby impact critical cellular functions, including transcription and repair. Further simulations and experimental studies are needed to explore this intriguing possibility. Preliminary studies (Y. Cai, I. Fu, et al., to be published) show that the same B[*a*]P-dG lesion placed at SHL ∼ −1 entraps the nearby H4 tail. Elegant experimental studies with nucleosome core particles in the Greenberg laboratory have shown that cross-links are formed between lysine residues in histone tails and DNA abasic lesions, and the extent of reaction depends on lesion position relative to the tails.[43,44] Understanding how structurally diverse lesions, their positioning on the nucleosome gyres with respect to the histone tails, and tail post-translational modifications impact the nucleosome stability, and the tail structures, dynamics, and biological functions, presents rich opportunities for future investigations.

DOI: 10.1021/acs.biochem.5b01166
Biochemistry XXXX, XXX, XXX−XXX

■ ASSOCIATED CONTENT

Supporting Information

The Supporting Information is available free of charge on the ACS Publications website at DOI: 10.1021/acs.biochem.5b01166.

Movie S1 (AVI)

Supplementary methods, tables, and figures (PDF)

■ AUTHOR INFORMATION

Corresponding Author

*E-mail: broyde@nyu.edu. Telephone: (212) 998-8231.

Funding

National Institutes of Health (NIH) (Grants CA-28038 to S.B., CA-168469 to N.E.G., and R01-GM079223 to Y.Z.). Computational infrastructure and systems management were partially supported by NIH Grant CA-75449 to S.B.

Notes

The authors declare no competing financial interest.

■ ACKNOWLEDGMENTS

This work used the Extreme Science and Engineering Discovery Environment (XSEDE), which is supported by National Science Foundation (NSF) Grant MCB060037 to S.B., as well as the computational resources provided by NYU-ITS.

■ ABBREVIATIONS

PTM, post-translational modification; BER, base excision repair; NER, nucleotide excision repair; MMS, methylmethanesulfonate; B[*a*]P, benzo[*a*]pyrene; B[*a*]P-dG, 10*S* (+)-*trans*-*anti*-B[*a*]P-N^2-dG; SHL, superhelical location; NCP, nucleosome core particle; Me, methyl group; NMR, nuclear magnetic resonance.

■ REFERENCES

(1) Bannister, A. J., and Kouzarides, T. (2011) *Cell Res. 21*, 381−395.
(2) Choudhary, C., Weinert, B. T., Nishida, Y., Verdin, E., and Mann, M. (2014) *Nat. Rev. Mol. Cell Biol. 15*, 536−550.
(3) Galvani, A., and Thiriet, C. (2015) *Genes 6*, 607−621.
(4) Bowman, G. D., and Poirier, M. G. (2015) *Chem. Rev. 115*, 2274−2295.
(5) Koprinarova, M., Schnekenburger, M., and Diederich, M. (2015) *Curr. Top. Med. Chem.* (Epub ahead of print).
(6) Zentner, G. E., and Henikoff, S. (2013) *Nat. Struct. Mol. Biol. 20*, 259−266.
(7) Taverna, S. D., Li, H., Ruthenburg, A. J., Allis, C. D., and Patel, D. J. (2007) *Nat. Struct. Mol. Biol. 14*, 1025−1040.
(8) Wyrick, J. J., and Parra, M. A. (2009) *Biochim. Biophys. Acta, Gene Regul. Mech. 1789*, 37−44.
(9) Verdone, L., Agricola, E., Caserta, M., and Di Mauro, E. (2006) *Briefings Funct. Genomics Proteomics 5*, 209−221.
(10) Kurdistani, S. K., and Grunstein, M. (2003) *Nat. Rev. Mol. Cell Biol. 4*, 276−284.
(11) Choi, J., Kim, H., Kim, K., Lee, B., Lu, W., and An, W. (2011) *Nucleic Acids Res. 39*, 9167−9180.
(12) Meas, R., Smerdon, M. J., and Wyrick, J. J. (2015) *Nucleic Acids Res. 43*, 4990−5001.
(13) Rodriguez, Y., Hinz, J. M., and Smerdon, M. J. (2015) *DNA Repair 32*, 113−119.
(14) Smerdon, M. J., Lan, S. Y., Calza, R. E., and Reeves, R. (1982) *J. Biol. Chem. 257*, 13441−13447.
(15) Guo, R. F., Chen, J., Mitchell, D. L., and Johnson, D. G. (2011) *Nucleic Acids Res. 39*, 1390−1397.
(16) Li, S. S. (2012) *Int. J. Mol. Sci. 13*, 12461−12486.
(17) Scharer, O. D. (2013) *Cold Spring Harbor Perspect. Biol. 5*, a012609.
(18) Grunstein, M. (1997) *Nature 389*, 349−352.
(19) Waters, R., van Eijk, P., and Reed, S. (2015) *DNA Repair 36*, 105−113.
(20) Glozak, M. A., and Seto, E. (2007) *Oncogene 26*, 5420−5432.
(21) Kuo, C. H., Hsieh, C. C., Lee, M. S., Chang, K. T., Kuo, H. F., and Hung, C. H. (2013) *Asia Pac. Allergy 4*, 14−18.
(22) Lee, J., Hwang, Y. J., Kim, K. Y., Kowall, N. W., and Ryu, H. (2013) *Neurotherapeutics 10*, 664−676.
(23) Grunstein, M. (1997) *Nature 389*, 349−352.
(24) Collepardo-Guevara, R., Portella, G., Vendruscolo, M., Frenkel, D., Schlick, T., and Orozco, M. (2015) *J. Am. Chem. Soc. 137*, 10205−10215.
(25) Nag, R., Kyriss, M., Smerdon, J. W., Wyrick, J. J., and Smerdon, M. J. (2010) *Nucleic Acids Res. 38*, 1450−1460.
(26) Parra, M. A., Kerr, D., Fahy, D., Pouchnik, D. J., and Wyrick, J. J. (2006) *Mol. Cell. Biol. 26*, 3842−3852.
(27) Cosman, M., de los Santos, C., Fiala, R., Hingerty, B. E., Singh, S. B., Ibanez, V., Margulis, L. A., Live, D., Geacintov, N. E., Broyde, S., and Patel, D. J. (1992) *Proc. Natl. Acad. Sci. U. S. A. 89*, 1914−1918.
(28) Geacintov, N. E., Cosman, M., Hingerty, B. E., Amin, S., Broyde, S., and Patel, D. J. (1997) *Chem. Res. Toxicol. 10*, 111−146.
(29) Mocquet, V., Kropachev, K., Kolbanovskiy, M., Kolbanovskiy, A., Tapias, A., Cai, Y., Broyde, S., Geacintov, N. E., and Egly, J. M. (2007) *EMBO J. 26*, 2923−2932.
(30) Berman, H. M., Westbrook, J., Feng, Z., Gilliland, G., Bhat, T. N., Weissig, H., Shindyalov, I. N., and Bourne, P. E. (2000) *Nucleic Acids Res. 28*, 235−242.
(31) Ong, M. S., Richmond, T. J., and Davey, C. A. (2007) *J. Mol. Biol. 368*, 1067−1074.
(32) Davey, C. A., Sargent, D. F., Luger, K., Maeder, A. W., and Richmond, T. J. (2002) *J. Mol. Biol. 319*, 1097−1113.
(33) Case, D. A., Darden, T. A., Cheatham, T. E., III, Simmerling, C. L., Wang, J., Duke, R. E., Luo, R., Walker, R. C., Zhang, W., Merz, K. M., Roberts, B., Wang, B., Hayik, S., Roitberg, A., Seabra, G., Kolossváry, I., Wong, K. F., Paesani, F., Vanicek, J., Liu, J., Wu, X., Brozell, S. R., Steinbrecher, T., Gohlke, H., Cai, Q., Ye, X., Wang, J., Hsieh, M. J., Cui, G., Roe, D. R., Mathews, D. H., Seetin, M. G., Sagui, C., Babin, V., Gusarov, S., Kovalenko, A., and Kollman, P. A. (2014) *AMBER 14*, University of California, San Francisco.
(34) Hornak, V., Abel, R., Okur, A., Strockbine, B., Roitberg, A., and Simmerling, C. (2006) *Proteins: Struct., Funct., Genet. 65*, 712−725.
(35) Perez, A., Marchan, I., Svozil, D., Sponer, J., Cheatham, T. E., 3rd, Laughton, C. A., and Orozco, M. (2007) *Biophys. J. 92*, 3817−3829.
(36) Jorgensen, W. L., Chandrasekhar, J., Madura, J. D., Impey, R. W., and Klein, M. L. (1983) *J. Chem. Phys. 79*, 926−935.
(37) Humphrey, W., Dalke, A., and Schulten, K. (1996) *J. Mol. Graphics 14*, 33−38.
(38) Plevin, M. J., Bryce, D. L., and Boisbouvier, J. (2010) *Nat. Chem. 2*, 466−471.
(39) Fratini, A. V., Kopka, M. L., Drew, H. R., and Dickerson, R. E. (1982) *J. Biol. Chem. 257*, 14686−14707.
(40) Flyvbjerg, H., and Petersen, H. G. (1989) *J. Chem. Phys. 91*, 461−466.
(41) Yang, W., Bitetti-Putzer, R., and Karplus, M. (2004) *J. Chem. Phys. 120*, 2618−2628.
(42) Horowitz, S., and Trievel, R. C. (2012) *J. Biol. Chem. 287*, 41576−41582.
(43) Sczepanski, J. T., Wong, R. S., McKnight, J. N., Bowman, G. D., and Greenberg, M. M. (2010) *Proc. Natl. Acad. Sci. U. S. A. 107*, 22475−22480.
(44) Weng, L., and Greenberg, M. M. (2015) *J. Am. Chem. Soc. 137*, 11022−11031.

DOI: 10.1021/acs.biochem.5b01166
Biochemistry XXXX, XXX, XXX−XXX